Polymer Chemistry

ROYAL SOCIETY OF CHEMISTRY

PAPER

View Article Online
View Journal | View Issue

Cite this: *Polym. Chem.*, 2025, **16**, 2943

Cyclobutane-linked nanothreads through thermal and photochemically mediated polymerization of cyclohexadiene†

Morgan Murphy,[a] Bohan Xu,[b] Katie E. Rank,[c] Sikai Wu,[a] Steven Huss,[a] John V. Badding,[a,b,d] Steven A. Lopez, [c] Vincent H. Crespi[a,b,d] and Elizabeth Elacqua *[a]

Carbon nanothreads are a rapidly growing class of 1D nanomaterials with sp^3-hybridized diamond-like backbones. They are typically synthesized through pressure-induced polymerizations of aromatics, resulting in diverse structures and functionalities. Aside from precursor selection, there are limited means to control reaction pathway or polymerization outcome. Analogous to selection rules that govern outcomes in molecular chemistry, we investigated thermally and photochemically mediated pressure-induced polymerizations of 1,4-cyclohexadiene and explored the resultant products. Thermally mediated polymerization of 1,4-cyclohexadiene yields a crystalline product; yet identification of the backbone architecture is complicated by the product's less ordered packing in which only two Friedel pairs are observed. Support for cyclobutane-based structures is present when comparing experimentally-obtained data to computed structures, yet further evidence suggesting eliptical cross-sections consistent with *anti*-cyclobutanes is obtained when comparing experimental data obtained from a Paris Edinburgh (PE) synthesis. In contrast, the recovered product obtained from the photochemically mediated polymerization exhibits different *d*-spacings and is consistent with simulations that support a single pathway toward highly elliptical *syn*-cyclobutane-linked nanothreads. These results suggest that photochemistry can enable reaction selectivity in nanothread synthesis.

Received 12th May 2025,
Accepted 19th May 2025

DOI: 10.1039/d5py00470e

rsc.li/polymers

Introduction

Pressure-induced polymerization of unsaturated precursors has often yielded amorphous hydrocarbon networks.[1–5] Recently, the high pressure polymerization of aromatic molecules realized a new class of materials – coined nanothreads – when the slow solid-state compression of benzene afforded a distinct crystalline product.[6,7] Nanothreads are synthesized through a pressure-induced polymerization[6–29] that leverages the kinetic control of the organic solid state to enable covalent bond formation along reactant stacks within a molecular crystal. NMR spectra obtained for benzene- and furan-derived nanothreads supported polymerization through repeated [4 + 2]-cycloadditions.[13,15] In contrast, cubane-derived nanothreads were the result of radical polymerization.[10] Whereas such reactions are dictated by the solid-state arrangement of precursor molecules,[17–23] methods to select specific reaction pathways and access new architectures remain largely unstudied.

In solution-based and solid-state organic synthesis, heat and light are often used to achieve different product and/or mechanistic outcomes. Orbital symmetry and the Woodward–Hoffmann selection rules dictate pericyclic reaction pathways[30] often enabling different products and/or stereoisomers under photochemical (*versus* thermal) conditions. Translating this concept to macromolecular systems, in particular carbon-based nanothreads, could enable different mechanisms and stereochemical outcomes to be achieved. Moreover, the use of photochemistry to direct nanothread formation may realize alternate architectures and/or facilitate reactivity.

Recently, photochemical irradiation was reported to reduce reaction pressures for nanothread formation.[9,31] Monomeric pyridine, for instance, formed well-ordered sp^3-rich products using laser or broadband irradiation. In the polymerization of furan, nanothread formation was also observed at reduced pressures; quantum mechanical calculations revealed that a photochemically allowed [4 + 4]-cycloaddition was favored as

[a]*Department of Chemistry, The Pennsylvania State University, University Park, PA, 16802, USA. E-mail: elizabeth.elacqua@psu.edu*
[b]*Department of Physics, The Pennsylvania State University, University Park, PA, 16802, USA*
[c]*Department of Chemistry and Chemical Biology, Northeastern University, Boston, MA, 02115, USA*
[d]*Department of Materials Science and Engineering, The Pennsylvania State University, University Park, PA, 16802, USA*

† Electronic supplementary information (ESI) available. See DOI: https://doi.org/10.1039/d5py00470e

the initiation step[9] in contrast to thermal polymerizations, thus enabling propagation through more energetically-favorable [4 + 2]-cycloadditions. While the introduction of light to access a structurally diverse array of 1D polymers is well-studied,[32–39] leveraging photochemistry to selectively dictate polymer structure (compared to thermal means) in strict analogy to molecular systems has yet to be documented.

Here, we investigate 1,3- and 1,4-cyclohexadiene as monomers for pressure-induced polymerization with the objective of interrogating non-aromatic compounds as new precursors toward sp^3-rich rigid polymers. We hypothesize the nature of the diene – conjugated or skipped – would dictate which polymerization mechanisms are viable, while expecting different pathways compared to benzene.[40] Previous dimerizations of 1,3-cyclohexadiene have reported observing a mixture of products; these results suggested that [2 + 2]-cycloaddition and [4 + 2]-cycloaddition were in direct competition.[41,42] Dimerizations of substituted 1,4-cyclohexadienes, although lesser studied, result predominantly in cyclobutane linkages.[43] In studies with these isomeric, yet structurally distinct monomers, we became interested in using our photochemical method[9] to investigate alternate reaction mechanisms and/or product formation, hypothesizing that heat and light mediated polymerizations likely afford different products with fewer accessible reaction pathways with light. Our hypotheses, while in analogy to molecular organic chemistry, contrast traditional polymerizations wherein heat and light are less known to dictate the resultant polymerization mechanism, and thus, polymer backbone.

Results and discussion

We hypothesized that 1,3-cyclohexadiene could polymerize through a series of [4 + 2]-cycloaddition reactions analogous to degree-4 nanothreads derived from aromatic precursors such as benzene and furan.[13,15] Whereas non-aromatic π-bond-containing molecules have not been explored, we envisioned that 1,3-cyclohexadiene's intrinsic conjugated s-*cis* diene, akin to furan, might enable facile nanothread formation through sequential [4 + 2]-cycloadditions.

Liquid 1,3-cyclohexadiene was loaded into a diamond anvil cell (DAC), where it solidified into an amorphous phase at approximately 1.5 GPa, as confirmed by a lack of lattice modes observed in the Raman spectrum (Fig. S1†). We studied the diene's thermal (20–22 °C) reactivity up to 21 GPa using *in situ* Raman and infrared (IR) spectroscopy. Attempts to polymerize 1,3-cyclohexadiene however, invariably achieved an amorphous C(sp^3)-rich product (see ESI†). We attributed the ill-defined product to competing pericyclic reactions which are both experimentally[41,42] and computationally supported.[44]

In contrast, 1,4-cyclohexadiene features a skipped diene, which would both disable [4 + 2]-cycloaddition pathways and likely favor cyclobutane products. Monomeric 1,4-cyclohexadiene may de facto realize new architectures from the pressure-induced polymerization. We calculated the reaction free energies associated with oligomerization through theoretical reactions (Fig. S30 and S31†) resulting in partially and fully saturated structures attainable through Zigzag (ZZ), Armchair (AC), and Cyclobutane (CB) pathways (Fig. 1). Our calculations suggested that propagating [2 + 2]-cycloadditions toward CB-linked structures was thermodynamically favorable when the reacting molecules of 1,4-cyclohexadiene are staggered. Further, radical mechanistic pathways toward AC or ZZ architectures were disfavored upon initiation (see ESI†).

The pressure-induced polymerization of 1,4-cyclohexadiene was first investigated up to 21 GPa at 20–22 °C in a DAC. We observed the broadening and shifting of C–H stretching modes at increased pressures using *in situ* IR spectroscopy (Fig. 2). All other vibrational modes broadened with increased pressure, while the sp^2 stretching modes decreased in intensity between 14 and 15 GPa. In the recovered spectrum at 0 GPa, stretching in the C–H sp^2 region shifted to lower wavenumbers (from 3054 to 3017 cm^{-1}) while sp^3 stretching modes from 2948 to 2881 cm^{-1} merged into a broad peak centered at 2917 cm^{-1}. New ring deformations at 886 cm^{-1} and new bending vibrations were seen at 620 and 953 cm^{-1} suggesting a new chemical environment in the product. Additional vibrational modes observed at 1035 and 1475 cm^{-1} likely corresponding to ring breathing modes, along with new sp^2–

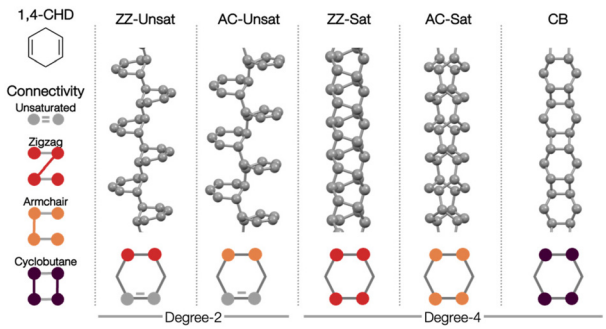

Fig. 1 Possible structural outcomes from a one-dimensional polymerization of 1,4-cyclohexadiene with different connectivity patterns.

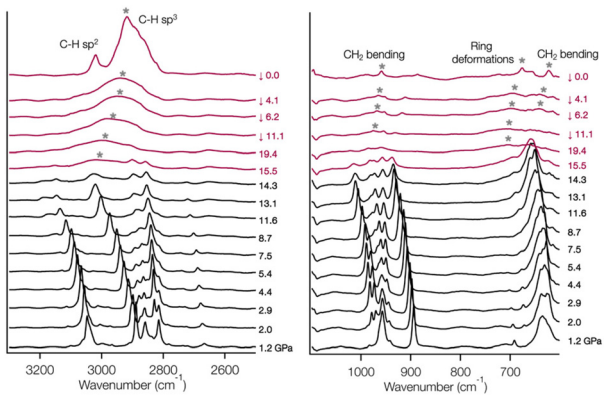

Fig. 2 *In situ* IR spectral overlay from the compression and decompression (↓) of 1,4-cyclohexadiene to 21 GPa. Asterisks denote new peaks.

sp^3 bending modes were observed, consistent with a reaction under pressure (Fig. S6†). Prominent HC═CH bending modes of 1,4-cyclohexadiene at 1160 cm^{-1} were absent in the recovered spectrum, indicating consumption of precursor. Additionally, IR spectroscopy of the recovered product suggested ~80% of the C-atoms are sp^3 hybridized (see ESI†).[2]

In a separate experiment, *in situ* Raman spectroscopy showed an increased PL background between 14 and 18 GPa (Fig. S5†), which is often indicative of a chemical change. This coincided with C–H broadening in the aforementioned IR spectroscopy experiment. After 24 hours at the maximum pressure, the sample was decompressed. A phase transition was seen with *in situ* Raman spectroscopy. This was supported by new vibrational modes appearing as low as 2.5 GPa, at which point the sample no longer matched the reported ambient pressure Raman spectra for 1,4-cyclohexadiene.[45] Synchrotron XRD of the recovered sample showed two interplanar spacings with $d_{24\text{-hour}}$ = 6.04 and 5.83 Å (Fig. 3).

In an *in situ* PXRD experiment, 1,4-cyclohexadiene was compressed to 21 GPa and held at that pressure for 96 hours to monitor the crystalline product. The reported low temperature crystal structure of 1,4-cyclohexadiene does not index to the high-pressure experimental sample above 4 GPa, suggesting a distinct high-pressure phase. With an unknown high-pressure molecular phase, we traced the XRD during decompression of the crystalline product. We recovered a product with two interplanar spacings ($d_{96\text{-hour}}$ = 6.14 Å and 4.90 Å (Fig. 3)) that suggested anisotropic packing (Fig. 4). We observed expansion of the interplanar spacings throughout decompression which was more pronounced over the last 2 GPa (Fig. 5).

Decompression data from the *in situ* XRD experiment (96-hour sample) was compared to the simulated diffraction of 1,4-cyclohexadiene-derived materials to gain insights into product formation. The simulated structures included both degree-2 (unsaturated (unsat)) and degree-4 (saturated (sat)) nanothreads of Zigzag (ZZ-unsat and ZZ-sat) and Armchair (AC-unsat and AC-sat) connectivity, along with cyclobutane (CB)-links, and crosslinked materials (see ESI† for all simulated structures and packings). Some categories of structural candidates were easily eliminated owing to disagreement between simulated and experimentally obtained *d*-spacings. For example, the simulated diffraction for sheet-like products (Fig. S27 and S28†) deviated significantly from the experimental decompression data; thus, structures of this dimensionality could be excluded.

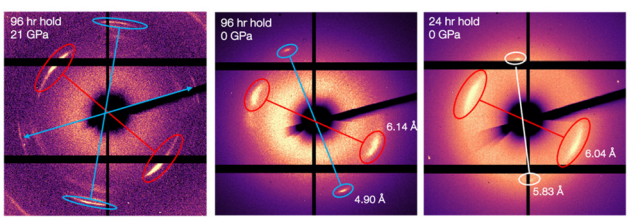

Fig. 3 Recovered gasket diffraction from experiments that polymerized at the max pressure for 96 hours and 24 hours.

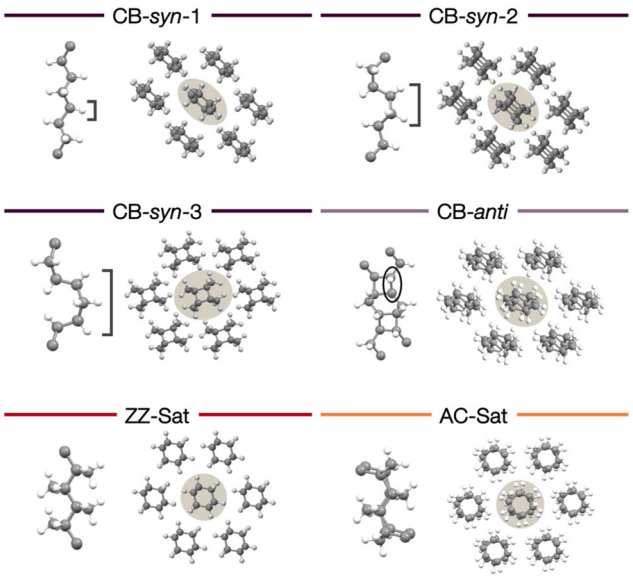

Fig. 4 Simulated structures and anisotropic packings relaxed at 0 K and 0 GPa. The number of consecutive hydrogens (shown with brackets) along the backbone is used to differentiate CB-*syn* packings. The *anti*-pair of hydrogens is circled.

The non-rigid unsaturated structures each have two distinct conformations (eclipsed and staggered); the unsaturated staggered conformations yielded one *d*-spacing exceeding 7.0 Å, which is excluded by experimental data. Unsaturated eclipsed conformations are more than 0.7 eV higher in enthalpy per precursor than staggered counterparts (which is not overcome by PΔV enthalpy differences at the reaction pressure). Furthermore, these two structures are conformational isomers and the eclipsed may convert to staggered at ambient conditions; thus, the eclipsed conformation was also ruled out.

To examine nanothread candidates, we assumed the observed reaction product Friedel pairs are associated with the two-dimensional lattice of thread packing, despite only seeing two of the expected three pairs; such peaks are typically more easily observed than those from axial periodicity and strong orientational order, presumably due to longer-ranged structural order in the packing direction.

The remaining thread candidates included CB-*syn*, CB-*anti*, ZZ-sat, and AC-sat structures (Fig. S29†). CB-*syn* threads would be formed from propagating [π2s + π2s]-cycloadditions which are traditionally understood as symmetry forbidden.[46] In contrast, CB-*anti* threads would arise from symmetry allowed [π2s + π2a]-cycloadditions. While they are 0.25–0.5 eV higher in enthalpy per precursor and more than 0.4 eV higher in gas phase dimerization barrier than CB-*syn* threads, this reaction would be symmetry-allowed under thermal conditions. The dimerization barrier is computed by slow-growth method implemented through VASP.[47–49] For simulated CB-*syn* structures, the number after the conformation indicates consecutive hydrogen pairs along one side of the backbone. For instance, CB-*syn*-3 has three consecutive hydrogen pairs, which accumu-

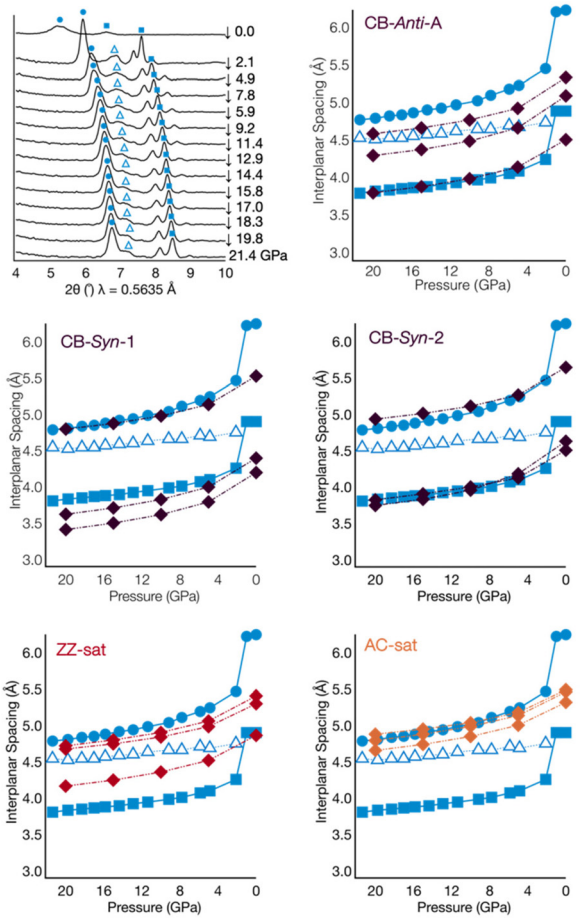

Fig. 5 Experimental (96-hour sample) and simulated X-ray diffraction data for the polymerization of 1,4-cyclohexadiene: (top left) overlay tracing decompression with blue circles, squares, and triangles highlighting relevant peaks and (top right, middle and bottom panels) comparison of experimental *d*-spacing to simulated diffraction data for different packings.

lates curvature that manifests as a more circular nanothread cross-section in projection along the axis (Fig. 4), similar to that of AC-Sat. In contrast, the lack of curvature in CB-*syn*-1 produces a more elliptical cross-section. Lastly, CB-*syn*-1 and CB-*anti* structures pack quite differently although both are overall elliptical. Moreover, given the steric constraints imposed by a [π2s + π2a]-cycloaddition, alignment and packing of curved *anti*-CB threads arising from such reactions might be expected to be ill-defined.

We compared the simulated diffraction data for these remaining structures with *in situ* XRD from decompression at 21 GPa (Fig. 5). Unmarked peaks at approximately 8° and 9° 2θ were attributed to precursor and not analyzed further. Those marked by solid blue circles and solid blue squares likely arise from the two-dimensional lattice of thread packing. The combination of a long (blue circle) and short (blue square) *d*-spacing indicated an ellipticity only achievable by CB-threads (Fig. 5). A weak set of Friedel pairs with the same *d*-spacing as the blue squares was observed at 21 GPa but not at ambient pressure. Having two sets of similarly spaced Friedel pairs is consistent with the CB-threads in simulations (Fig. 5). A weak broader peak marked with a hollow blue triangle, which is close to a peak of the precursor molecular crystal, disappeared at ambient pressure. Its variation in *d*-spacing under decompression also differs from those *d*-spacings associated of with thread packing. Therefore, this hollow triangle peak was not included in analysis of thread packings.

Considering the solid circle and square peaks, the *d*-spacings from the 96-hour sample matched well, at all pressures, with simulated CB-threads (Fig. 8), although the absence of the expected third *d*-spacing complicates absolute assignment. The abrupt expansion on decompression is characteristic of other nanothreads[16] and is attributed to release of pressure-induced straightening of the threads around on-thread structural defects (the disorder associated with this "destraightening" may account for the unobservability of all *d*-spacings upon recovery). Moreover, XRD obtained on the 24-hour sample (Fig. 3) similarly only showed two Friedel pairs and lacked a second long or short *d*-spacing. Although both CB-based threads and AC-sat threads align best with observed *d*-spacings, the absence of an expected third set of quasi-hexagonal Friedel pairs prevents a more confident identification of its reaction product.

We conducted a synthesis in the Paris Edinburgh (PE) press that mimicked the 24-hour experiment (*i.e.*, the sample was held at the maximum pressure for 24 hours). The cyclohexadiene-derived solid produced in a PE press showed a strong diffraction, with *d*-spacings of 5.78 and 4.94 Å (see Fig. S34†). This sample similarly lacked the expected third *d*-spacing; this consistent observation of only two interplanar spacings may be the signature of products that experience ill-defined (and perhaps inconsistent) packing unlike conventional nanothreads whose structures are poly(adamantane)-like and more rigid. Considering that the thermal experiments do not follow any different synthetic protocols, aside from the time held at the maximum pressure, the combined experiments (Table 1) suggest convergence on an elliptical product with one short and two long interplanar spacings, with each experiment resulting in two of those being defined in the resultant XRD. This convergence also matches with the cyclobutane product whose stereochemical outcome is consistent with the symmetry-allowed [π2s + π2a]-trajectory, thus enabling a more confident ruling out of other [2 + 2]-dimerization-based products.

Overall, the thermally mediated polymerization of 1,4-cyclohexadiene supports the formation of an elliptical product whose packing appears to be ill-defined in comparison to

Table 1 Summary of *d*-spacings arising from thermal experiments, both in a DAC and PE press

24-hour (DAC)	96-hour (DAC)	24-hour (PE press)
6.04 Å	6.14 Å	—
5.83 Å	—	5.76 Å
—	4.90 Å	4.94 Å

other nanothreads that pack more densely. The combined data supports the formation of cyclohexadiene-based nanothreads with architectures supporting either the CB-*anti* or ZZ-sat product by way of pericyclic and radical-type mechanisms, respectively. Of the two, the CB-*anti* threads have a closer match between experiment and simulated structures; we do note, however, that the low symmetry of the CB-*anti* threads and overall high enthalpies may enable multiple slightly different packings. Moreover, optimized oligomer structures (see ESI†) indicate some degree of curvature that would support less dense packings. In contrast, we will show that the photochemically mediated reaction affords an ordered thread that features all expected Friedel pairs, along with a highly elliptical cross-section associated with CB-*syn*-threads that arise from a single reaction pathway.

To explore photochemical reaction pathways, and/or reduce reaction pressures, polycrystalline 1,4-cyclohexadiene was compressed and irradiated using a high-pressure mercury lamp (HBO103 W/2, OSRAM) in a DAC. Several conditions were tested, varying maximum pressure and exposure time (see ESI†). The optimal experiments reached a maximum pressure of 18 GPa, then were exposed to UV light in three one-hour increments with Raman scans taken immediately after each exposure (Fig. 6). Spectra showed broadening of diene vibrational modes under pressure and a slight increase in PL background at the maximum pressure. After each UV light exposure, the PL background increased significantly, likely due to chemical transformation. IR spectra of the recovered solid featured an intense C–H stretching peak below 3000 cm^{-1} (Fig. S7†), along with new vibrational modes at 1035 and 1475 cm^{-1} which likely correspond to a ring breathing mode and new sp^2–sp^3 bending modes. Collectively, these observations suggested that the sample underwent a successful reaction.

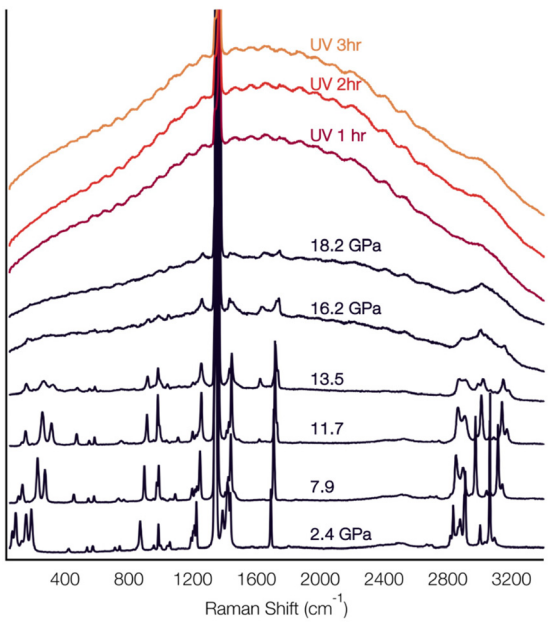

Fig. 6 *In situ* Raman spectral overlay of the photochemically mediated compression of 1,4-cyclohexadiene to 18 GPa and subsequent Raman scans after each 1-hour irradiation period.

Synchrotron X-ray diffraction of recovered gasket samples showed a pseudo-hexagonal diffraction pattern with *d*-spacings belonging to the nanothread lattice at 6.24, 5.04, and 4.86 Å (Fig. 7). Recent photochemically mediated nanothread syntheses saw a reduction in reaction pressure but yielded the same or very similar *d*-spacings as/to those of non-irradiated samples.[9,31] Here, the introduction of photochemistry did reduce the reaction pressure, but also resulted in a product with *d*-spacings that were distinct from those obtained through thermal compressions.

These *d*-spacings were compared to the simulated candidate structures and packings (Fig. 7). The observation of one large and two smaller *d*-spacings in the experimental data reflects elliptical cross-sections, suggesting that CB-*syn* linkages were the reaction product. The experimental diffraction showed three Friedel pairs for first-order diffraction spots of a quasi-hexagonal thread packing, in contrast to the thermal reaction product. Thus, an increase in structural order – which

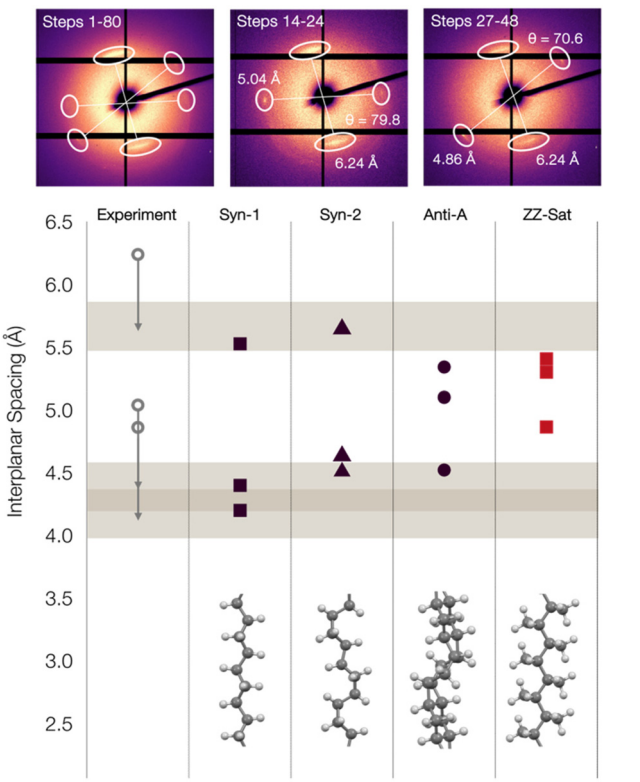

Fig. 7 Synchrotron X-ray diffraction of 1,4-cyclohexadiene compressed to 18 GPa with 3 hours of UV light (accumulation of steps 80 scans highlighting Friedel pairs (scans 14–24 and 27–48)) and comparison of experimental and simulated *d*-spacings. A 0.5–0.8 Å (decreasing) shift was applied to the photochemical *d*-spacings to compare to the theoretically obtained *d*-spacings; this shift accounts for both destraightening and thermal expansion that is observed upon decompression in the non-irradiated experiments (see main text). The shaded bands represent the 0.3 Å range of uncertainty.

might arise from higher symmetry *syn*-cyclobutanes – was obtained under photochemical conditions. Moreover, the photochemical reaction product also lacked the ~5.8 Å peak observed in the thermal reaction (Table 1, DAC and PE press 24-hour experiments). The combined data suggested that photochemical conditions selected a singular mechanistic pathway toward cyclobutane formation, while thermal conditions – which still favors cyclobutanes by achieving the [π2s + π2a]-trajectory – may also enable a radical-mediated pathway (Fig. 8). In contrast, the single cyclobutane-forming pathway was favored under photochemical conditions owing to the Woodward–Hoffmann allowed [π2s + π2s]-pathway.

The "destraightening" seen upon pressure release for thermally produced threads was expected to also impact the photochemical synthesis. Given the absence of thermal expansion within the theoretical thread packings (and the inability to experimentally monitor the photochemical decompression), we applied a 0.5–0.8 Å (decreasing) shift to the experimentally obtained *d*-spacings for the photochemical sample. This value comes from the expansion observed upon decompression in the thermal experiments (Fig. 7) and enables treatment of the data obtained from both methods in the same manner when comparing to the defect-free thread packings at 0 GPa. With this correction, the experimental *d*-spacings were consistent with the simulated CB-linked *syn*-1 and *syn*-2 threads. The stereochemistry of these threads (*i.e.*, *cis*-hydrogens along the backbone) indicated that the light mediated polymerization promoted [π2s + π2s]-cycloadditions in construction of the polymer backbone. This cycloaddition is favored by both strain minimization and orbital symmetry under photochemical conditions. Thus, the use of photochemistry to mediate the polymerization of 1,4-cyclohexadiene selected for a single pericyclic-based reaction pathway resulting in a more well-defined cyclobutane-based nanothread when compared to the thermal polymerization (Fig. 8).

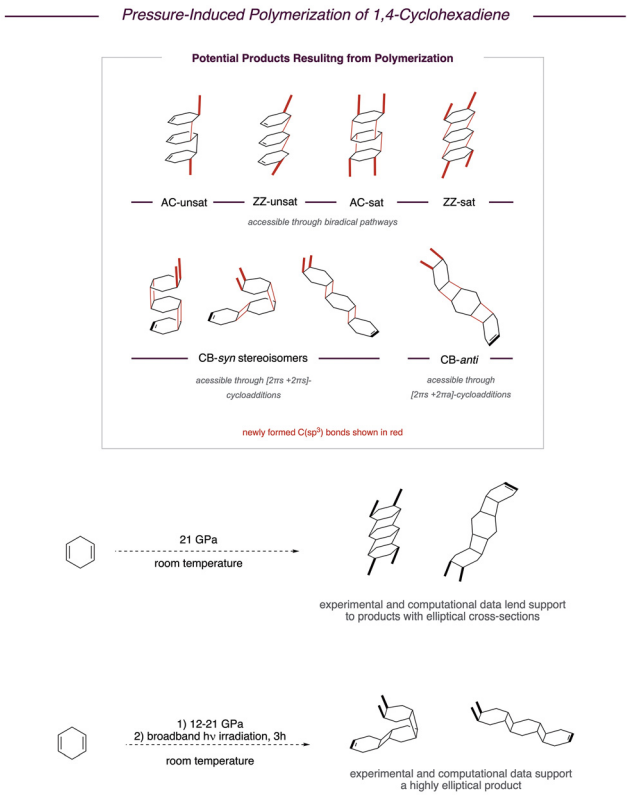

Fig. 8 Summation of 1,4-cyclohexadiene polymerization, including (top) overall accessible products, and (bottom) proposed structures obtained from thermal and photochemically mediated experiments. Propagation sites are bolded for clarity on proposed bond formations.

Conclusions

Herein, we disclose the synthesis of cyclobutane-linked nanothreads, derived from the non-aromatic sp^2-rich precursor cyclohexadiene. Both 1,3- and 1,4-cyclohexadiene are separately compressed at ambient temperature, affording sp^3-enriched polymers; however, only the skipped diene ultimately achieves products that are one-dimensional and crystalline, likely owing to fewer viable reaction pathways. X-ray diffraction obtained on products of thermal activation invariably demonstrates only two visible interplanar spacings ($d_{24\text{-hour}}$ = 5.83 and 6.04 Å, $d_{96\text{-hour}}$ = 4.90 and 6.14 Å, and $d_{\text{PE-press}}$ = 4.98 and 5.78 Å), suggesting that the threads formed do not have consistent packing modes. Combined, the 24-hour experiments within the DAC and PE press afford two different, yet complementary pairs that suggest the major product arising from thermal polymerization pathways demonstrates elliptical cross-sections with one shorter and two larger interplanar spacings. Comparison to simulated structures supports fully saturated products with *anti*-CB linkages being most plausible, although zigzag arrangements cannot be fully ruled out. The reactivity of 1,4-cyclohexadiene was further investigated using UV light, wherein a single reaction pathway emerged: an architecture that propagated through solely [π2s + π2s]-cycloadditions was favored, as evidenced by three experimentally observed Friedel pairs (d_{photo} = 4.86, 5.04, and 6.24 Å) that correlated with a highly elliptical cross-section achieved by successive cyclobutane formation. The combined provides strong support for the photochemically mediated polymerization of 1,4-cyclohexadiene having enabled a single reaction pathway to be selected, in contrast to thermal methods which may access both pericyclic and radical-based mechanisms.

The ability to utilize both thermal and photochemical activation modes to impact mechanism and potentially control chemical reactivity under pressure has significant implications for polymer backbone design. Moreover, the integration of non-aromatics into kinetically controlled polymerizations enables a rich variety of hydrocarbon-based materials to be discovered based on commodity chemicals and natural resources. While we demonstrate the light's ability to dictate reaction mechanism – in contrast to more viable reaction pathways arising from thermal polymerization – we expect many sp^2-rich non-aromatic precursors to demonstrate preferential

reactivities under pressure, consistent with traditional organic synthesis.

Author contributions

E. E. conceived the idea and, with V. H. C., designed the project. M. M., S. W., and S. H. conducted all experiments and collected data. B. X. and K. E. R., performed all theoretical studies and collected data. All authors analyzed both experimental and computational data. All authors helped with preparing and revising the manuscript. M. M. and E. E. prepared the ESI† and all authors revised them.

Data availability

All experimental data are provided in the ESI.† All Gaussian16 files are uploaded to the open-access repository, figshare, accessible through: **doi.org/10.6084/m9.figshare.26018272.v2**.

Conflicts of interest

There are no conflicts to declare.

Acknowledgements

This work was partially funded by the Center for Nanothread Chemistry, a National Science Foundation (NSF) Center for Chemical Innovation (CHE-1832471). Partial support for this project is also through the NSF MRSEC SEED program (DMR-2011839). E. E. acknowledges support in the form of an Alfred P. Sloan Foundation grant FG-2021-15490. S. A. L. and K. E. R. thank the NSF for financial support (NSF-OAC-2118201). Portions of this work were performed at HPCAT (Sector 16), Advanced Photon Source (APS), Argonne National Laboratory. HPCAT operations are supported by DOE-NNSA's Office of Experimental Sciences. The Advanced Photon Source is a U.S. Department of Energy (DOE) Office of Science User Facility operated for the DOE Office of Science by Argonne National Laboratory under Contract No. DE-AC02-06CH11357. We thank Guoyin Shen and Changyong Park for their assistance with XRD measurements. This research used 22-IR-1 at the National Synchrotron Light Source II, a U.S. DOE Office of Science User Facility operated for the DOE Office of Science by Brookhaven National Laboratory under Contract No. DE-SC0012704. We thank Zhenxian Liu for assistance with collecting IR spectral data. The XRD used to analyze PE press samples was supported by SIG S10 of the National Institutes of Health (award numbers 1S100D028589-01 and 1S10RR023439-01 to Dr. Yennawar). We thank Dr. Hee Jeung Oh and Luis Thiele for assistance with DSC measurements. Additionally, we would like to thank Shweta Gaikwad for assistance with GC-MS measurements.

References

1 V. Schettino and R. Bini, Constraining molecules at the closest approach: chemistry at high pressure, *Chem. Soc. Rev.*, 2007, **36**, 869–880.
2 L. Ciabini, M. Santoro, R. Bini and V. Schettino, High pressure reactivity of solid benzene probed by infrared spectroscopy, *J. Chem. Phys.*, 2002, **116**, 2928–2935.
3 M. Citroni, R. Bini, P. Foggi and V. Schettino, Role of excited electronic states in the high-pressure amorphization of benzene, *Proc. Natl. Acad. Sci. U. S. A.*, 2008, **105**, 7658–7663.
4 P. Pruzan, J. C. Chervin, M. M. Thiéry, J. P. Itié, J. M. Besson, J. P. Forgerit and M. Revault, Transformation of benzene to a polymer after static pressurization to 30 GPa, *J. Chem. Phys.*, 1990, **92**, 6910–6915.
5 M. Ceppatelli, M. Santoro, R. Bini and V. Schettino, High pressure reactivity of solid furan probed by infrared and Raman spectroscopy, *J. Chem. Phys.*, 2003, **118**, 1499–1506.
6 T. C. Fitzgibbons, M. Guthrie, E.-S. Xu, V. H. Crespi, S. K. Davidowski, G. D. Cody, N. Alem and J. V. Badding, Benzene-derived carbon nanothreads, *Nat. Mater.*, 2015, **14**, 43–47.
7 X. Li, M. Baldini, T. Wang, B. Chen, E.-S. Xu, B. Vermilyea, V. H. Crespi, R. Hoffmann, J. J. Molaison, C. A. Tulk, M. Guthrie, S. Sinogeikin and J. V. Badding, Mechanochemical Synthesis of Carbon Nanothread Single Crystals, *J. Am. Chem. Soc.*, 2017, **139**, 16343–16349.
8 X. Li, T. Wang, P. Duan, M. Baldini, H.-T. Huang, B. Chen, S. J. Juhl, D. Koeplinger, V. H. Crespi, K. Schmidt-Rohr, R. Hoffmann, N. Alem, M. Guthrie, X. Zhang and J. V. Badding, Carbon Nitride Nanothread Crystals Derived from Pyridine, *J. Am. Chem. Soc.*, 2018, **140**, 4969–4972.
9 S. M. Oburn, S. Huss, J. Cox, M. C. Gerthoffer, S. Wu, A. Biswas, M. Murphy, V. H. Crespi, J. V. Badding, S. A. Lopez and E. Elacqua, Photochemically Mediated Polymerization of Molecular Furan and Pyridine: Synthesis of Nanothreads at Reduced Pressures, *J. Am. Chem. Soc.*, 2022, **144**, 22026–22034.
10 H.-T. Huang, L. Zhu, M. D. Ward, T. Wang, B. Chen, B. L. Chaloux, Q. Wang, A. Biswas, J. L. Gray, B. Kuei, G. D. Cody, A. Epshteyn, V. H. Crespi, J. V. Badding and T. A. Strobel, Nanoarchitecture through Strained Molecules: Cubane-Derived Scaffolds and the Smallest Carbon Nanothreads, *J. Am. Chem. Soc.*, 2020, **142**, 17944–17955.
11 D. Gao, X. Tang, J. Xu, X. Yang, P. Zhang, G. Che, Y. Wang, Y. Chen, X. Gao, X. Dong, H. Zheng, K. Li and H.-K. Mao, Crystalline $C_3N_3H_3$ tube (3,0) nanothreads, *Proc. Natl. Acad. Sci. U. S. A.*, 2022, **119**, e2201165119.
12 T. Wang, P. Duan, E.-S. Xu, B. Vermilyea, B. Chen, X. Li, J. V. Badding, K. Schmidt-Rohr and V. H. Crespi, Constraining Carbon Nanothread Structures by Experimental and Calculated Nuclear Magnetic Resonance Spectra, *Nano Lett.*, 2018, **18**, 4934–4942.
13 P. Duan, X. Li, T. Wang, B. Chen, S. J. Juhl, D. Koeplinger, V. H. Crespi, J. V. Badding and K. Schmidt-Rohr, The

Chemical Structure of Carbon Nanothreads Analyzed by Advanced Solid-State NMR, *J. Am. Chem. Soc.*, 2018, **140**, 7658–7666.

14 A. Biswas, M. D. Ward, T. Wang, L. Zhu, H.-T. Huang, J. V. Badding, V. H. Crespi and T. A. Strobel, Evidence for Orientational Order in Nanothreads Derived from Thiophene, *J. Phys. Chem. Lett.*, 2019, **10**, 7164–7171.

15 B. S. Matsuura, S. Huss, Z. Zheng, S. Yuan, T. Wang, B. Chen, J. V. Badding, D. Trauner, E. Elacqua, A. C. T. van Duin, V. H. Crespi and K. Schmidt-Rohr, Perfect and Defective ^{13}C-Furan-Derived Nanothreads from Modest-Pressure Synthesis Analyzed by ^{13}C NMR, *J. Am. Chem. Soc.*, 2021, **143**, 9529–9542.

16 S. Huss, S. Wu, B. Chen, T. Wang, M. C. Gerthoffer, D. J. Ryan, S. E. Smith, V. H. Crespi, J. V. Badding and E. Elacqua, Scalable Synthesis of Crystalline One-Dimensional Carbon Nanothreads through Modest-Pressure Polymerization of Furan, *ACS Nano*, 2021, **15**, 4134–4143.

17 S. G. Dunning, B. Chen, L. Zhu, G. D. Cody, S. Chariton, V. B. Prakapenka, D. Zhang and T. A. Strobel, Synthesis and Post-Processing of Chemically Homogeneous Nanothreads from 2,5-Furandicarboxylic Acid, *Angew. Chem., Int. Ed.*, 2023, **62**, e202217023.

18 S. G. Dunning, L. Zhu, B. Chen, S. Chariton, V. B. Prakapenka, M. Somayazulu and T. A. Strobel, Solid-State Pathway Control via Reaction-Directing Heteroatoms: Ordered Pyridazine Nanothreads through Selective Cycloaddition, *J. Am. Chem. Soc.*, 2022, **144**, 2073–2078.

19 W. S. Tang and T. A. Strobel, Evidence for Functionalized Carbon Nanothreads from π-Stacked, para-Disubstituted Benzenes, *J. Phys. Chem. C*, 2020, **124**, 25062–25070.

20 X. Wang, X. Yang, Y. Wang, X. Tang, H. Zheng, P. Zhang, D. Gao, G. Che, Z. Wang, A. Guan, J.-F. Xiang, M. Tang, X. Dong, K. Li and H.-K. Mao, From Biomass to Functional Crystalline Diamond Nanothread: Pressure-Induced Polymerization of 2,5-Furandicarboxylic Acid, *J. Am. Chem. Soc.*, 2022, **144**, 21837–21842.

21 M. D. Ward, W. S. Tang, L. Zhu, D. Popov, G. D. Cody and T. A. Strobel, Controlled Single-Crystalline Polymerization of $C_{10}H_8{\cdot}C_{10}F_8$ under Pressure, *Macromolecules*, 2019, **52**, 7557–7563.

22 A. Friedrich, I. E. Collings, K. F. Dziubek, S. Fanetti, K. Radacki, J. Ruiz-Fuertes, J. Pellicer-Porres, M. Hanfland, D. Sieh, R. Bini, S. J. Clark and T. B. Marder, Pressure-Induced Polymerization of Polycyclic Arene–Perfluoroarene Cocrystals: Single Crystal X-ray Diffraction Studies, Reaction Kinetics, and Design of Columnar Hydrofluorocarbons, *J. Am. Chem. Soc.*, 2020, **142**, 18907–18923.

23 M. C. Gerthoffer, S. Wu, B. Chen, T. Wang, S. Huss, S. M. Oburn, V. H. Crespi, J. V. Badding and E. Elacqua, 'Sacrificial' supramolecular assembly and pressure-induced polymerization: toward sequence-defined functionalized nanothreads, *Chem. Sci.*, 2020, **11**, 11419–11424.

24 M. C. Gerthoffer, B. Xu, S. Wu, J. Cox, S. Huss, S. M. Oburn, S. A. Lopez, V. H. Crespi, J. V. Badding and E. Elacqua, Mechanistic insights into the pressure-induced polymerization of aryl/perfluoroaryl co-crystals, *Polym. Chem.*, 2022, **13**, 1359–1368.

25 W. S. Tang and T. A. Strobel, Pressure-Induced Solid-State Polymerization of Optically-Tunable Diphenyl-Substituted Diacetylene, *ACS Appl. Polym. Mater.*, 2019, **1**, 3286–3294.

26 S. Romi, S. Fanetti, F. Alabarse, A. M. Mio, J. Haines and R. Bini, Towards custom built double core carbon nanothreads using stilbene and pseudo-stilbene type systems, *Nanoscale*, 2022, **14**, 4614–4625.

27 M. M. Nobrega, E. Teixeira-Neto, A. B. Cairns, M. L. A. Temperini and R. Bini, One-dimensional diamondoid polyaniline-like nanothreads from compressed crystal aniline, *Chem. Sci.*, 2018, **9**, 254–260.

28 S. Fanetti, M. Santoro, F. Alabarse, B. Enrico and R. Bini, Modulating the H-bond strength by varying the temperature for the high pressure synthesis of nitrogen rich carbon nanothreads, *Nanoscale*, 2020, **12**, 5233–5242.

29 M. Agati, S. Romi, S. Fanetti and R. Bini, High-pressure structure and reactivity of crystalline bibenzyl: Insights and prospects for the synthesis of functional double-core carbon nanothreads, *J. Chem. Phys.*, 2023, **159**, 244507.

30 R. Hoffmann and R. B. Woodward, Selection Rules for Concerted Cycloaddition Reactions, *J. Am. Chem. Soc.*, 1965, **87**, 2046–2048.

31 H. Su, X. Li, C. Ye, C. Gao, X. Sun, Z. Wang, R. Dai and Z. Zhang, Confirmation of Phase Transitions and Laser-Assisted Chemical Reaction for Pyridine under High Pressure, *J. Phys. Chem. C*, 2022, **126**, 12536–12544.

32 D.-F. Chen, S. Bernsten and G. M. Miyake, Organocatalyzed Photoredox Radical Ring-Opening Polymerization of Functionalized Vinylcyclopropanes, *Macromolecules*, 2020, **53**, 8352–8359.

33 D.-F. Chen, B. M. Boyle, B. G. McCarthy, C.-H. Lim and G. M. Miyake, Controlling Polymer Composition in Organocatalyzed Photoredox Radical Ring-Opening Polymerization of Vinylcyclopropanes, *J. Am. Chem. Soc.*, 2019, **141**, 13268–13277.

34 M. Chen, M. J. MacLeod and J. A. Johnson, Visible-Light-Controlled Living Radical Polymerization from a Trithiocarbonate Iniferter Mediated by an Organic Photoredox Catalyst, *ACS Macro Lett.*, 2015, **4**, 566–569.

35 V. K. Kensy, R. L. Tritt, F. M. Haque, L. M. Murphy, D. B. Knorr Jr, S. M. Grayson and A. J. Boydston, Molecular Weight Control via Cross Metathesis in Photo-Redox Mediated Ring-Opening Metathesis Polymerization, *Angew. Chem., Int. Ed.*, 2020, **59**, 9074–9079.

36 V. Kottisch, Q. Michaudel and B. P. Fors, Cationic Polymerization of Vinyl Ethers Controlled by Visible Light, *J. Am. Chem. Soc.*, 2016, **138**, 15535–15538.

37 K. A. Ogawa, A. E. Goetz and A. J. Boydston, Metal-Free Ring-Opening Metathesis Polymerization, *J. Am. Chem. Soc.*, 2015, **137**, 1400–1403.

38 R. M. Pearson, C.-H. Lim, B. G. McCarthy, C. B. Musgrave and G. M. Miyake, Organocatalyzed Atom Transfer Radical Polymerization Using N-Aryl Phenoxazines as Photoredox Catalysts, *J. Am. Chem. Soc.*, 2016, **138**, 11399–11407.

39 J. Xu, S. Shanmugam, C. Fu, K.-F. Aguey-Zinsou and C. Boyer, Selective Photoactivation: From a Single Unit Monomer Insertion Reaction to Controlled Polymer Architectures, *J. Am. Chem. Soc.*, 2016, **138**, 3094–3106.
40 B. Chen, T. Wang, V. H. Crespi, X. Li, J. Badding and R. Hoffmann, All the Ways To Have Substituted Nanothreads, *J. Chem. Theory Comput.*, 2018, **14**, 1131–1140.
41 D. Valentine, N. J. Turro and G. S. Hammond, Thermal and Photosensitized Dimerizations of Cyclohexadiene, *J. Am. Chem. Soc.*, 1964, **86**, 5202–5208.
42 F.-G. Klärner, B. M. J. Dogan, O. Ermer, W. V. E. Doering and M. P. Cohen, Mechanism of the Thermal 1,3-Cyclohexadiene Dimerization: A Non-Concerted Diels-Alder Reaction Leading to the exo-[4 + 2] Adduct and a Novel [6 + 4]-Ene Reaction, *Angew. Chem., Int. Ed. Engl.*, 1986, **25**, 108–110.
43 G. Ahlgren and B. Åkermark, Photodimerisation of 1,4-cyclohexadiene-1,2-dicarboxylic anhydride, *Tetrahedron Lett.*, 1974, **15**, 987–988.
44 B. Chen, K. N. Houk and R. Cammi, High-Pressure Reaction Profiles and Activation Volumes of 1,3-Cyclohexadiene Dimerizations Computed by the Extreme Pressure-Polarizable Continuum Model (XP-PCM), *Chem. – Eur. J.*, 2022, **28**, e202200246.
45 H. Hagemann, H. Bill, D. Joly, P. Müller and N. Pautex, Raman investigation of 1,4-cyclohexadiene in the liquid and solid state, *Spectrochim. Acta, Part A*, 1985, **41**, 751–756.
46 R. B. Woodward and R. Hoffmann, The Conservation of Orbital Symmetry, *Angew. Chem., Int. Ed. Engl.*, 1969, **8**, 781–853.
47 C. Jarzynski, Nonequilibrium Equality for Free Energy Differences, *Phys. Rev. Lett.*, 1997, **78**, 2690–2693.
48 T. K. Woo, P. M. Margl, P. E. Blöchl and T. Ziegler, A Combined Car–Parrinello QM/MM Implementation for ab Initio Molecular Dynamics Simulations of Extended Systems: Application to Transition Metal Catalysis, *J. Phys. Chem. B*, 1997, **101**, 7877–7880.
49 H. Oberhofer, C. Dellago and P. L. Geissler, Biased Sampling of Nonequilibrium Trajectories: Can Fast Switching Simulations Outperform Conventional Free Energy Calculation Methods?, *J. Phys. Chem. B*, 2005, **109**, 6902–6915.